Chapter 8
Disturbance Observer Based Control: Aerospace Applications

The practical implementation of sliding mode controllers usually assumes knowledge of all system states. It also typically requires information (at least in terms of the boundaries) about the combined effect of drift terms, i.e., the internal and external disturbances of the system. In this chapter a feedback linearization-like technique is used for obtaining the input–output dynamics and reducing all disturbances to the matched ones. Then the sliding variables are introduced and their dynamics are derived. The higher-order sliding mode differentiator-based observer, which was discussed in Chap. 7, is used to the estimate system states, the derivatives of the sliding variables, as well as the drift terms. Therefore, in finite time, all information about the sliding variable dynamics becomes available. The estimated drift term is then used in the feedback loop to compensate the disturbances. The observed states are then used to design any (continuous) robust state-space controller while eliminating the chattering effect. Two case studies, launch vehicle and satellite formation control, illustrate the discussed robust control technique.

8.1 Problem Formulation

This section presents a continuous SMC technique based on a sliding mode disturbance observer (SMDO) that is applied to robust output tracking in feedback-linearizable perturbed/uncertain MIMO systems, with nonlinear feedback. Consider a nonlinear MIMO system

$$\begin{aligned} \dot{x} &= f(x,t) + G(x,t)u \\ y &= h(x,t) \end{aligned} \tag{8.1}$$

where $f(x,t), \in \mathbb{R}^n$, $h(x,t) = [h_1, h_2, \ldots, h_m]^T \in \mathbb{R}^m$, $G(x,t) = [g_1, g_2, \ldots, g_m] \in \mathbb{R}^{n\times m}$, and $g_i \in \mathbb{R}^n \ \forall i = 1, 2, \ldots, m$ are analytic vector and matrix functions. The system states, outputs, and inputs are given by $x \in \mathbb{R}^n$, $y \in \mathbb{R}^m$, and $u \in \mathbb{R}^m$,

Y. Shtessel et al., *Sliding Mode Control and Observation*, Control Engineering,
DOI 10.1007/978-0-8176-4893-0_8,

respectively. Assume that the system (8.1) is completely feedback linearizable in a reasonable compact domain $x \in \Omega$. Then the system can be transformed into a regular form

$$\begin{bmatrix} y_1^{(r_1)} \\ y_2^{(r_2)} \\ \dots \\ y_m^{(r_m)} \end{bmatrix} = \begin{bmatrix} L_f^{r_1} h_1(x,t) \\ L_f^{r_2} h_2(x,t) \\ \dots \\ L_f^{r_m} h_m(x,t) \end{bmatrix} + E(x,t)u \tag{8.2}$$

where

$$E(x,t) = \begin{bmatrix} L_{g_1}(L_f^{r_1-1}h_1) & L_{g_2}(L_f^{r_1-1}h_1) & \dots & L_{g_m}(L_f^{r_1-1}h_1) \\ L_{g_1}(L_f^{r_2-1}h_2) & L_{g_2}(L_f^{r_2-1}h_2) & \dots & L_{g_m}(L_f^{r_2-1}h_2) \\ \dots & \dots & \dots & \dots \\ L_{g_1}(L_f^{r_m-1}h_m) & L_{g_2}(L_f^{r_m-1}h_m) & \dots & L_{g_m}(L_f^{r_m-1}h_m) \end{bmatrix} \tag{8.3}$$

and $\det E(x,t) \neq 0$. In the above $L_f^{r_i} h_i(x,t)$ and $L_{g_i}(L_f^{r_j-1}h_j)$ $\forall i,j = 1,2,\dots,m$ are the corresponding Lie derivatives. The vector $\bar{r} = [r_1, r_2, \dots, r_m]$ is the vector-relative degree, and $r_t = \sum r_i$ is the total relative degree, such that $r_t = n$.

The problem is in designing a continuous control u that provides robust decoupled output tracking in system (8.1):

$$e_i = y_{ic} - y_i \to 0 \quad \forall i = 1,2,\dots,m \tag{8.4}$$

where y_{ic} is the i^{th} output command profile given online.

The formulated problem is addressed by enforcing the desired compensated dynamics. This is achieved by designing corresponding sliding variables, driving them to zero by means of continuous sliding mode controls u_i.

8.1.1 Asymptotic Compensated Dynamics

In this subsection the sliding variables is introduced as

$$\sigma_i = e_i^{(r_i-1)} + c_{i,r_i-2}e_i^{(r_i-2)} + \dots + c_{i,1}e_i^{(1)} + c_{i,0}e_i, \; i = 1,2,\dots m \tag{8.5}$$

The asymptotic decoupled output tracking compensated dynamics in system (8.2), such that $e_i \to 0$ $\forall i = 1,2,\dots m$ is achieved in the sliding mode

$$e_i^{(r_i-1)} + c_{i,r_i-2}e_i^{(r_i-2)} + \dots + c_{i,1}e_i^{(1)} + c_{i,0}e_i = 0 \; \forall i = 1,2,\dots m \tag{8.6}$$

if the coefficients $c_{i,j} > 0 \ \forall j = 0, 1, .., r_i - 2$ are chosen to provide the desired eigenvalue placement in the decoupled differential equations (8.6). The dynamics in Eq. (8.6) is enforced by designing control u that drives $\sigma_i \to 0$.

8.1.2 Finite-Time-Convergent Compensated Dynamics

In this subsection the sliding variables are chosen to guarantee the finite-time-convergent compensated dynamics in the sliding mode. They are:

$$e_i^{(r_i)} + k_{i,r_i} \left| e_i^{(r_i-1)} \right|^{\alpha_{i,r_i}} \text{sign}\left(e_i^{(r_i-1)}\right) + \ldots + k_{i,1} |e_i|^{\alpha_{i,1}} \text{sign}(e_i) = 0 \ \ \forall i = 1, 2, \ldots m \tag{8.7}$$

where the coefficients $k_{i,j} > 0 \ \forall i = 1, 2, \ldots m \ \ \forall j = 1, 2, \ldots r_i$, make the polynomials $P_i(\lambda) = (\lambda^{r_i} + k_{i,r_i}\lambda^{r_i-1} + \ldots + k_{i,1}$ Hurwitz, and $\alpha_{i,1}, \ldots, \alpha_{i,r_i}$ are defined as

$$\alpha_{i,j-1} = \frac{\alpha_{i,j}\alpha_{i,j+1}}{2\alpha_{i,j+1} - \alpha_{i,j}} \ \forall i = 1, 2, \ldots m \ \forall j = 2, 3, \ldots r_i \tag{8.8}$$

with $\alpha_{i,r_i+1} = 1$ and $\alpha_{i,r_i} = \alpha$ for some $\alpha \in (0, 1)$.

The compensated dynamics (8.7) and (8.8) can be enforced by designing an appropriate continuous control u.

Remark 8.1. In order to compute the sliding variable σ_i given by Eq. (8.5) or to enforce the finite-convergent-time asymptotic dynamics in Eqs. (8.7) and (8.8) the $r_i - 1$ consecutive derivatives of the tracking error e_i must be calculated/estimated. This can be achieved using the HOSM differentiator studied in Chaps. 4 and 6:

$$\begin{aligned}
\dot{z}_{0i} &= v_{0i} = z_{1i} - \kappa_{0i} |z_{0i} - e_i|^{\frac{r_i}{r_i+1}} \text{sign}(z_{0i} - e_i) \\
\dot{z}_{1i} &= v_{1i} = z_{2i} - \kappa_{1i} |z_{1i} - v_{0i}|^{\frac{r_i-1}{r_i}} \text{sign}(z_{1i} - v_{0i}) \\
&\ldots \\
\dot{z}_{r_i,i} &= -\kappa_{r_i,i} \text{sign}(z_{r_i,i} - v_{r_i-1,i})
\end{aligned} \tag{8.9}$$

where the κ_{ji} are defined as in Sect. 6.7. The finite-time estimation of the output tracking errors and their consecutive $r_i - 1$ derivatives $e_i, \ldots, e_i^{(r_i-1)}$ can be easily obtained from equations $z_{0i} = e_i, z_{1i} = \dot{e}_i, .., z_{r_i-1,i} = e_i^{(r_i-1)}$.
Denoting

$$v = E(x,t)u \Leftrightarrow u = E^{-1}(x,t)v, \ v = [v_1, v_2, .., v_m]^T \tag{8.10}$$

the sliding variable (8.5) dynamics can be presented in a decoupled form

$$\dot{\sigma}_i = \psi_i(.) - v_i \tag{8.11}$$

where $\psi_i(.) = y_{ic}^{(r_i)} - L_f^{r_i} h_i(x,t) + c_{i,r_i-2} e^{(r_i-1)} + \ldots + c_{i,0} e^{(1)} \ \forall i = 1, 2, \ldots m.$

Remark 8.2. In order to facilitate the computation of the matrix $E^{-1}(x,t)$ the state vector x must be estimated in finite time. In particular, it can be achieved using HOSM observers (see Chap. 7).

8.1.3 Sliding Variable Disturbed Dynamics

Assume that the drift terms $\psi_i(.)$ in Eq. (8.11) consist of a sum of known terms $\psi_i^0(.)$ and the unknown terms $\Delta\psi_i(.)$:

$$\psi_i(.) = \psi_i^0(.) + \Delta\psi_i(.) \tag{8.12}$$

The unknown terms that are due to external disturbances and model uncertainties are assumed to be bounded so that $|\Delta\psi_i(.)| \leq L_i$.

Then, Eq. (8.11) can be rewritten in a form

$$\dot{\sigma}_i = \psi_i^0(.) + \Delta\psi_i(.) - v_i \tag{8.13}$$

Now, the output tracking problem in system (8.2) is reduced to designing the continuous control laws v_i that drive the sliding variables σ_i to zero in the presence of the unknown bounded disturbances $\Delta\psi_i(.)$.

8.1.4 Output Tracking Error Disturbed Dynamics

In order to design the controller that drives the tracking errors to zero in finite time, the error dynamics (8.4) for system (8.2) are presented as

$$e_i^{(r_i)} = y_{ic}^{(r_i)} - L_f^{r_i} h_i(x,t) - v_i \tag{8.14}$$

where $\bar{\psi}_i(.) = y_{ic}^{(r_i)} - L_f^{r_i} h_i(x,t)$ can be presented as a sum of known $\bar{\psi}_i^0(.)$ and unknown bounded $\left|\Delta\bar{\psi}_i(.)\right| \leq \bar{L}_i$ terms:

$$\bar{\psi}_i(.) = \bar{\psi}_i^0(.) + \Delta\bar{\psi}_i(.) \tag{8.15}$$

Therefore, the error dynamics in Eq. (8.14) are reduced to the following equation:

$$e_i^{(r_i)} = \bar{\psi}_i^0(.) + \Delta\bar{\psi}_i(.) - v_i \tag{8.16}$$

Here the problem is reduced to designing the continuous control laws v_i that drive the output tracking errors in Eq. (8.16) to zero in *finite time* in the presence of the unknown bounded disturbances $\Delta\bar{\psi}_i(.)$.

8.2 Perturbation Term Reconstruction via a Disturbance Observer

In the first step of the continuous SMC/SMDO design methodology, the perturbation term must be estimated/reconstructed.

In order to design the SMDO for estimating the bounded disturbance $\Delta\psi_i(.)$ in Eq. (8.13), the auxiliary sliding variables s_i are introduced

$$s_i = \sigma_i + z_i \tag{8.17}$$

$$\dot{z}_i = -\psi_i^0(.) + v_i - \omega_i \tag{8.18}$$

whose dynamics are derived as

$$\frac{\mathrm{d}s_i}{\mathrm{d}t} = \Delta\psi_i(.) - \omega_i \tag{8.19}$$

where ω_i is the injection term of the SMDO in Eq. (8.19).

For estimating the bounded disturbance $\Delta\bar{\psi}_i(.)$ in Eq. (8.16), other auxiliary sliding variables $\bar{s}_i$ are introduced:

$$\bar{s}_i = e_i^{(r_i-1)} + \xi_i \tag{8.20}$$

$$\dot{\xi}_i = -\bar{\psi}_i^0(.) + v_i - \varpi_i \tag{8.21}$$

The $\bar{s}_i$ dynamics, taking into account Eq. (8.16), are presented as

$$\frac{\mathrm{d}\bar{s}_i}{\mathrm{d}t} = \Delta\bar{\psi}_i(.) - \varpi_i \tag{8.22}$$

where ϖ_i is the injection term of the SMDO in Eq. (8.22).

8.2.1 SMDO Based on Conventional SMC

The injection term given in a conventional SMC format is

$$\omega_i = \rho_i \,\mathrm{sign}(s_i), \quad \rho_i = L_i + \varepsilon_i \tag{8.23}$$

which drives $s_i \to 0$ in finite time. Then, in the auxiliary sliding mode, $s_i = 0$; and the disturbance term $\Delta\psi_i(.)$ can be exactly estimated:

$$\Delta\psi_i(.) = \omega_{i_{eq}} \tag{8.24}$$

where $\omega_{i_{eq}}$ is the equivalent injection term. Note that it is practically impossible to compute the equivalent injection term $\omega_{i_{eq}}$ exactly, but only estimate it via low-pass filtering of control (8.23) in the sliding mode. For instance, the low-pass filter can be implemented as a first-order lag block

$$\bar{\tau}_i \frac{\mathrm{d}\bar{\omega}_{i_{eq}}}{\mathrm{d}t} = -\bar{\omega}_{i_{eq}} + \omega_i \tag{8.25}$$

where $\bar{\tau}_i > 0$ is a small-enough time constant of the low-pass filter (8.25). It is worth noting that the low-pass filter estimates the equivalent injection term $\hat{\omega}_{i_{eq}}(t)$ with the accuracy proportional to the time constant of the filter $\hat{\tau}_i$:

$$\left\| \bar{\omega}_{i_{eq}} - \omega_{i_{eq}} \right\| = O(\bar{\tau}_i) \tag{8.26}$$

Therefore, we obtain the estimation of the perturbation term $\Delta\psi_i(.)$ in a conventional sliding mode

$$\Delta\psi_i(.)_{est} \approx \bar{\omega}_{i_{eq}} \tag{8.27}$$

with the accuracy

$$\|\Delta\psi_i(.)_{est} - \Delta\psi_i(.)\| = O(\bar{\tau}_i) \tag{8.28}$$

Furthermore, the $\lim \|\Delta\psi_i(.)_{est} - \Delta\psi_i(.)\| = 0$ as $\bar{\tau}_i \to 0$.

Remark 8.3. Since the term $\Delta\bar{\psi}_i(.)$ can be estimated by the conventional SMC-based SMDO only asymptotically, some phase and amplitude distortions are expected (see, for instance, Eq. (8.28)). Apparently, it is better not to reconstruct the term $\Delta\bar{\psi}_i(.)$ using this asymptotic observer for enforcing the output error dynamics in Eqs. (8.7) and (8.8), since these output tracking dynamics are expected to be finite-time convergent. Consequently, it makes sense to reconstruct the disturbance terms $\Delta\bar{\psi}_i(.)$ also in finite time in order to retain overall finite-time convergence (dynamical collapse) in the output tracking.

8.2.2 SMDO Based on Super-Twisting Control

Assuming the derivatives of the perturbation terms $\Delta\psi_i(.)$ in Eq. (8.19) are bounded, i.e., $\left|\frac{d\Delta\psi_i(.)}{dt}\right| \leq \bar{L}_i$, the injection terms given in a super-twisting format are

$$\begin{aligned} \omega_i &= \lambda_{0,i}|s_i|^{1/2}\mathrm{sign}(s_i) + \eta_i \\ \dot{\eta}_i &= \lambda_{1,i}\mathrm{sign}(s_i) \end{aligned} \tag{8.29}$$

with $\lambda_{0,i} = 1.5\sqrt{\tilde{L}_i}$ and $\lambda_{1,i} = 1.1\tilde{L}_i$ which drive $s_i, \dot{s}_i \to 0$ in finite time (see, for instance, Chaps. 4 and 7). Therefore, in the second-order sliding mode, an exact estimate of the perturbation term $\Delta\psi_i(.)$

$$\Delta\psi_i(.)_{est} = \omega_i \tag{8.30}$$

is obtained. The super-twisting-based SMDO can be also designed for estimating/reconstructing the unknown disturbances $\Delta\bar{\psi}_i(.)$ in Eq. (8.16), assuming that the derivative of this term is also bounded: i.e., $\left|\frac{d\Delta\bar{\psi}_i(.)}{dt}\right| \leq \tilde{L}_i$. The injection terms ϖ_i are designed in the super-twist format as in Eq. (8.29) so that

$$\begin{aligned} \varpi_i &= \beta_{0,i}|\bar{s}_i|^{1/2}\text{sign}(\bar{s}_i) + \chi_i \\ \dot{\chi}_i &= \beta_{1,i}\text{sign}(\bar{s}_i) \end{aligned} \tag{8.31}$$

with $\beta_{0,i} = 1.5\sqrt{\tilde{L}_i}$ and $\beta_{1,i} = 1.1\tilde{L}_i$ and drive $\bar{s}_i, \frac{d\bar{s}_i}{dt} \to 0$ in finite time. Thus, the disturbances $\Delta\bar{\psi}_i(.)$ are exactly reconstructed in finite time in accordance with Eq. (8.22) and the super-twisting SMDO (8.31):

$$\Delta\bar{\psi}_i(.)_{est} = \varpi_i$$

8.2.3 *Design of the SMC Driven by the SMDO*

Asymptotic Continuous SMC/SMDO Design

The continuous sliding mode controllers v_i driven by the sliding mode disturbance observer (SMC/SMDO) that robustly asymptotically stabilize the sliding variable σ_i, whose dynamics are given by Eq. (8.13) in the presence of an unknown bounded disturbance $\Delta\psi_i(.)$, are designed as follows:

$$v_i = \psi_i^0(.) + \Delta\psi_i(.)_{est} + K_i\sigma_i \tag{8.32}$$

The compensated sliding variable dynamics become

$$\dot{\sigma}_i = -K_i\sigma_i \tag{8.33}$$

where $K_i > 0$ must be selected in order to provide the desired convergence rate $\sigma_i \to 0$.

Therefore, a continuous control law u that robustly drives the output tracking error of Eq. (8.1) $e_i \to 0\ \forall i = 1, 2, \ldots m$ as time increases, in the presence of bounded disturbances, is designed given by

$$\begin{aligned} u &= E^{-1}(x,t)v, \quad v = [v_1, v_2, .., v_m]^T \\ v_i &= \psi_i^0(.) + \Delta\psi_i(.)_{est} + K_i\sigma_i\ \forall i = 1, 2, \ldots m \end{aligned} \tag{8.34}$$

where the $\Delta\psi_i(.)_{est}$ is estimated by either a conventional sliding mode or super-twisting SMDO. The sliding variables σ_i are computed using HOSM differentiators (8.9).

Remark 8.4. The SMC/SMDO design in Eqs. (8.27), (8.30), and (8.34) yields continuous control that is robust to the bounded disturbances and uncertainties. This SMC/SMDO controller can be interpreted as asymptotic SMC since $\sigma_i \to 0$ as time increases due to Eqs. (8.33) and (8.6).

Finite-Convergent-Time Continuous SMC/SMDO Design

The continuous sliding mode controllers v_i, driven by the sliding mode disturbance observer (SMC/SMDO), which robustly establish the error dynamics in Eq. (8.16) to zero in finite time are designed taking into account Eq. (8.7):

$$v_i = \bar{\psi}_i^0(.) + \Delta\bar{\psi}_i(.)_{est} + k_{i,r_i}\left|e_i^{(r_i-1)}\right|^{\alpha_{i,r_i}} \text{sign}\left(e_i^{(r_i-1)}\right) + \ldots + k_{i,1}\,|e_i|^{\alpha_{i,1}}\,\text{sign}\,(e_i) \tag{8.35}$$

The compensated finite-convergent-time output tracking error dynamics become as in Eq. (8.7).

Therefore, the continuous control law u that robustly drives the output tracking error e_i of Eq. (8.1) to zero in finite time in the presence of bounded disturbances is

$$u = E^{-1}(x,t)v \tag{8.36}$$

8.3 Case Study: Reusable Launch Vehicle Control

Flight control of both current and future reusable launch vehicles (RLV) in ascent and descent, as well as in approach and landing modes, involves attitude maneuvering through a wide range of flight conditions, wind disturbances, and plant uncertainties. The discussed SMC/SMDO becomes an attractive robust control algorithm for RLV maneuvers because, as well as being continuous, the SMC/SMDO controller is insensitive and robust to RLV uncertainties and external disturbances. In this section we study SMC/SMDO controller design for RLV flying in the terminal area energy management (TAEM) and approach/land (TAL) regions of flight (Fig. 8.1).

8.3.1 Mathematical Model of Reusable Launch Vehicle

The nonlinear Newton–Euler equations of motion for the rigid vehicle were chosen for the RLV flight control system design. The rotational equations of motion are

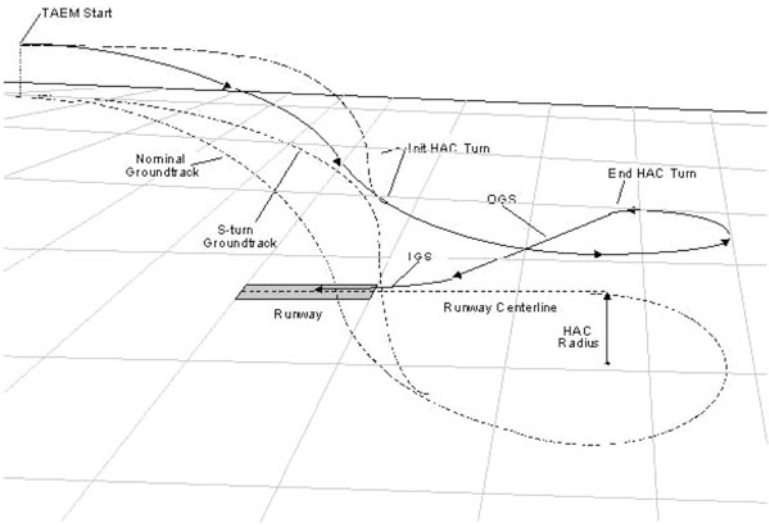

Fig. 8.1 Example TAEM and approach/land trajectory for a RLV [104]

$$\begin{aligned}\dot{p} &= -L_{pq}pq - L_{qr}qr + L + f_L \\ \dot{q} &= -M_{pr}pr - M_{r^2p^2}(r^2 - p^2) + M + f_M \\ \dot{r} &= -N_{pq}pq - N_{qr}qr + N + f_N\end{aligned} \tag{8.37}$$

where p, q, and r are the roll, pitch, and yaw rates, respectively; L_{pq}, L_{qr}, M_{pr}, $M_{r^2p^2}$, N_{pq}, and N_{qr} are functions of the vehicle inertia, L, M, and N are roll, pitch, and yaw accelerations arising from the aerodynamics, and f_L, f_M, and f_N are disturbance accelerations. Translational accelerations $(\dot{u}, \dot{v}, \dot{w})$ in the vehicle body frame are presented as:

$$\begin{aligned}\dot{u} &= rv - qw + X + G_x \\ \dot{v} &= pw - ru + Y + G_y \\ \dot{w} &= qu - pv + Z + G_z\end{aligned} \tag{8.38}$$

where the acceleration terms X, Y, and Z are from the aerodynamics and G_x, G_y, and G_z are gravity terms given by

$$G_x = -g\sin(\theta),\ G_y = g\cos(\theta)\sin(\phi),\ G_z = g\cos(\theta)\cos(\phi) \tag{8.39}$$

The Euler angles that define the orientation of the RLV relative to an inertial frame are

$$\begin{bmatrix} \dot{\phi} \\ \dot{\theta} \\ \dot{\psi} \end{bmatrix} = \begin{bmatrix} 1 & \tan(\theta)\sin(\phi) & \tan(\theta)\cos(\phi) \\ 0 & \cos(\phi) & -\sin(\phi) \\ 0 & \frac{\sin(\phi)}{\cos(\theta)} & \frac{\cos(\phi)}{\cos(\theta)} \end{bmatrix} \begin{bmatrix} p \\ q \\ r \end{bmatrix} \tag{8.40}$$

where ϕ, θ, and ψ are the roll, pitch, and yaw angles, respectively. The aerodynamic surfaces for the RLV are represented by three virtual surfaces (aileron, elevator, and rudder). The commanded virtual deflections

$$\delta_c = [\delta_{ac}, \delta_{ec}, \delta_{rc}]^T \tag{8.41}$$

where the subscripts a, e, and r represent aileron, elevator, and rudder, respectively, are distributed by a control allocator (CA) to actual aero surface actuator commands

$$\bar{\delta}_c = \left[\delta_{elc}, \delta_{erc}, \delta_{flc}, \delta_{frc}, \delta_{rlc}, \delta_{rrc}\right]^T \tag{8.42}$$

where the subscripts el, er, fl, fr, rl, and rr represent left and right elevons, left and right flaps, and left and right rudders, respectively. These commands are fed into the individual aero surface actuators, modeled here by first-order systems

$$\tau_i \dot{\delta}_i = \delta_{ic} - \delta_i, \quad i = el, er, fl, fr, rl, rr \tag{8.43}$$

The actual deflection angles in Eq. (8.43) are δ_i, the actuator time constants are τ_i, and the actuator command inputs are δ_{ic}.

Remark 8.5. The aero surface actuator models in Eq. (8.43) are simplifications of the actual models, which are of higher order and nonlinear. Modeling them as simple, linear first order as in Eq. (8.43) simplifies the controller design. In the simulations used to verify the design, the actuators were modeled as second-order systems with the following position and rate limits:

$$\begin{aligned} &-30^\circ \le \delta_i \le 25^\circ, \ \left|\dot{\delta}_i\right| \le 30\,\text{deg/s}, \ i = el, er \\ &-15^\circ \le \delta_j \le 26^\circ, \ \left|\dot{\delta}_j\right| \le 10\,\text{deg/s}, \ j = fl, fr \\ &-30^\circ \le \delta_{rl} \le 60^\circ, \ \left|\dot{\delta}_{rl}\right| \le 30\,\text{deg/s} \\ &-60^\circ \le \delta_{rr} \le 30^\circ, \ \left|\dot{\delta}_{rr}\right| \le 30\,\text{deg/s} \end{aligned}$$

8.3.2 Reusable Launch Vehicle Control Problem Formulation

The general problem for the flight control system design during TAL, is to determine aero surface deflection commands such that the guidance commands are robustly asymptotically followed, in the presence of external disturbances and uncertainties in the plant. Guidance commands in the TAL flight are N_{zc}, normal acceleration

(or $A_{zc} = -N_{zc}$ in terms of the body frame acceleration command), ϕ_c, roll angle, and r_c, yaw rate. The RLV mathematical model (8.37)–(8.40) is presented in a quasi-cascade format:

$$\begin{bmatrix} \dot{A}_z \\ \dot{\phi} \end{bmatrix} = \begin{bmatrix} \dot{v} & -\dot{u} \\ 1 & \tan(\theta)\sin(\phi) \end{bmatrix} \begin{bmatrix} p \\ q \end{bmatrix} + \begin{bmatrix} f_{Az} \\ f_{\phi} \end{bmatrix} \tag{8.44}$$

$$\begin{bmatrix} \dot{p} \\ \dot{q} \end{bmatrix} = \begin{bmatrix} -L_{pq}\, pq - L_{qr}\, qr \\ -M_{pr}\, pr - M_{r^2p^2}(r^2 - p^2 \end{bmatrix} + \begin{bmatrix} L \\ M \end{bmatrix} + \begin{bmatrix} f_L \\ f_M \end{bmatrix} \tag{8.45}$$

$$\dot{r} = -N_{pq}\, pq - N_{qr} qr + N + f_N \tag{8.46}$$

where the f_{ϕ}, f_{Az} are bounded disturbances ($|f_{\phi}| \leq L_{\phi}$, $|f_{Az}| \leq L_{Az}$) in the normal acceleration and roll channels. The term f_{ϕ} is caused by modeling errors, while f_{Az} comprises modeling errors and external disturbances, and f_L, f_M, and f_N are the disturbances in the roll rate, the pitch rate channels, and the yaw rate channel. All disturbances are bounded in a reasonable flight domain.

The goal is to design a continuous SMC/SMDO controller that provides decoupled asymptotic output tracking, i.e., $A_z \to A_{zc}, \phi \to \phi_c$, and $r \to \bar{r}_c$ as time increases, in the presence of bounded disturbances, by means of roll, pitch, and yaw acceleration commands L_c, M_c, and N_c.

8.3.3 Multiple-Loop Asymptotic SMC/SMDO Design

The control problem is addressed using the continuous SMC–SMDO algorithm in a multiple-loop format. The controller is designed in the following steps:

Step 1 A control law for the outer loop that drives $A_z \to A_{zc}$ and $\phi \to \phi_c$ is designed in terms of virtual rate commands, p_c, q_c, that are fed into the inner loop.

Step 2 A control law for the inner loop that drives $e_L = p \to p_c, q \to q_c$, and $r \to \bar{r}_c r_c + r_{cSAS}$, where $\bar{r}_c = r_c + r_{cSAS}$ and r_{cSAS} is a special term generated by the stability augmentation system (SAS), is designed in terms of angular accelerations, L_c, M_c, and N_c.

Step 3 A control allocation matrix $\mathbf{B}_A$ is used to map the angular acceleration command vector to the actuator virtual deflection commands:

$$\boldsymbol{\delta}_c = \mathbf{B}_A \mathbf{I} \begin{bmatrix} L_c \\ M_c \\ N_c \end{bmatrix}, \quad \boldsymbol{\delta}_c = [\delta_{ac}, \delta_{lc}, \delta_{rc}] \in \mathbb{R}^3, \ \mathbf{B}_A \in \mathbb{R}^{3\times 3}, \ \mathbf{I} \in \mathbb{R}^3 \tag{8.47}$$

CA is then used to distribute the virtual actuator commands $\boldsymbol{\delta}_c$ to actual aero surface actuator commands $\bar{\boldsymbol{\delta}}_c$, which are fed to the individual actuators (8.43): specifically

$$\bar{\boldsymbol{\delta}}_c = CA(\boldsymbol{\delta}_c), \quad \bar{\delta}_c = \left[\delta_{elc}, \delta_{erc}, \delta_{flc}, \delta_{frc}, \delta_{rlc}, \delta_{rrc}\right]^T \tag{8.48}$$

Outer-Loop SMC/SMDO Controller Design

The virtual controls, p_c and q_c , are designed in the following way:

$$\begin{bmatrix} p_c \\ q_c \end{bmatrix} = \begin{bmatrix} \dot{v} & -\dot{u} \\ 1 & \tan(\theta)\sin(\phi) \end{bmatrix}^{-1} \begin{bmatrix} \hat{d}_{Az} + K_{Az}\sigma_{Az} \\ \hat{d}_{\phi} + K_{\phi}\sigma_{\phi} \end{bmatrix} \tag{8.49}$$

where

$$\begin{aligned} \sigma_i &= e_i,\ i = A_z, \phi, \\ e_{Az} &= A_{zc} - A_z, e_{\phi} = \phi_c - \phi \end{aligned} \tag{8.50}$$

and $\hat{d}_{Az}$ is the estimate of $d_{Az} = \dot{A} - f_{Az}$, and $\hat{d}_{\phi}$ is the estimate of $d_{\phi} = \dot{\phi}_{Ac} - f_{\phi}$. Assuming $|d_{Az}| \leq \bar{L}_{Az}$, and $\left|d_{\phi}\right| \leq \bar{L}_{\phi}$ in a reasonable flight envelope, and denoting

$$\begin{bmatrix} \lambda_{Az} \\ \lambda_{\phi} \end{bmatrix} = \begin{bmatrix} \dot{v} & -\dot{u} \\ 1 & \tan(\theta)\sin(\phi) \end{bmatrix} \begin{bmatrix} p \\ q \end{bmatrix} \tag{8.51}$$

the finite-convergence-time SMDO based on a super-twisting injection term is designed, in accordance with Eqs. (8.17), (8.19), (8.23), (8.24), (8.25), and (8.27).

Firstly, auxiliary sliding variables are introduced as

$$s_i = \sigma_i + z_i,\ \dot{z}_i = \lambda_i - v_i,\ i = A_z, \phi \tag{8.52}$$

and the auxiliary sliding variable dynamics are derived as

$$\dot{s}_i = d_i - v_i,\ \ i = A_z, \phi \tag{8.53}$$

Secondly, the super-twisting injection terms that drive the auxiliary sliding variables $s_i, i = A_z, \phi$ to zero in finite time are designed (see Sect. 8.2.2)

$$\begin{aligned} v_i &= \lambda_{0,i} |s_i|^{1/2} \operatorname{sign}(s_i) + \eta_i \\ \dot{\eta}_i &= \lambda_{1,i} \operatorname{sign}(s_i) \end{aligned} \tag{8.54}$$

with $\lambda_{0,i} = 1.5\sqrt{\bar{L}_i}, \lambda_{1,i} = 1.1\bar{L}_i$. The auxiliary injection terms v_{A_z} and $v_{A\phi}$ exactly estimate the disturbances d_{A_z} and $d_{A\phi}$ in Eq. (8.53) in finite times, i.e.,

$$d_{A_z} = v_{A_z},\ d_{A\phi} = v_{A\phi} \tag{8.55}$$

The obtained disturbance estimates are substituted into the virtual control laws in Eq. (8.49).

Inner-Loop SMC/SMDO Controller Design

The inner-loop input–output dynamics are taken as the lower part of Eq. (8.46). The inner-loop SMC/SMDO takes the body rate virtual control commands, p_c and q_c, generated by the outer-loop controller (8.51)–(8.55), and the yaw rate command r_c that comes from the guidance function. The inner-loop continuous SMC/SMDO controller is supposed to enforce following the body rate virtual control commands in the presence of bounded disturbances and by generating pitch, roll, and yaw acceleration commands L_c, M_c, and N_c. In addition to tracking virtual body rate commands, the inner loop causes the system to exhibit a linear decoupled motion in the sliding mode. No timescale (separation) between the inner- and outer-loop compensated dynamics is required (but it is welcome). Following the continuous SMC/SMDO controller design algorithm presented above, the components of the vector-sliding variable are introduced as

$$\begin{aligned} &\sigma_i = e_i,\ i = L, M, N \\ &e_L = p_c - p,\ e_M = q_c - q,\ e_N = e_{SAS} \end{aligned} \tag{8.56}$$

where, in order to provide turn coordination, a SAS generates a yaw rate command

$$r_{cSAS} = \frac{g}{U}\sin(\phi) \tag{8.57}$$

where g is the gravitational constant, U is true air speed, and the error signal used in the yaw rate loop SMC/SMDO is

$$e_{sas} = (r_c + r_{cSAS} - r) \tag{8.58}$$

In the sliding mode $\sigma_L = \sigma_M = \sigma_N = 0$, and the inner-loop compensated error dynamics are decoupled. The objective of the inner-loop control is to generate continuous commands L_c, M_c, and N_c that provide asymptotic convergence of $\sigma_L, \sigma_M, \sigma_N \to 0$. The pitch, roll, and yaw acceleration control commands L_c ,M_c , and N_c are designed:

$$\begin{bmatrix} Lc \\ M_c \\ N_c \end{bmatrix} = \begin{bmatrix} \tilde{f}_L \\ \tilde{f}_M \\ \tilde{f}_N \end{bmatrix} + \begin{bmatrix} L_{pq} + L_{qr} qr \\ M_{pr} + M_{r^2p^2}(r^2 - p^2) \\ N_{pq} pq + N_{qr} qr \end{bmatrix} + \begin{bmatrix} K_L & 0 & 0 \\ 0 & K_M & 0 \\ 0 & 0 & K_N \end{bmatrix} \begin{bmatrix} \sigma_L \\ \sigma_M \\ \sigma_N \end{bmatrix} \tag{8.59}$$

where $\begin{bmatrix} \tilde{f}_L & \tilde{f}_M & \tilde{f}_N \end{bmatrix}^T$ is the estimate vector of the bounded accumulated disturbance

$$\begin{bmatrix} \bar{f}_L \\ \bar{f}_M \\ \bar{f}_N \end{bmatrix} = \begin{bmatrix} \dot{p}_c - f_L \\ \dot{q}_c - f_M \\ \dot{r}_c - f_N \end{bmatrix}$$

Assuming $\left|\bar{f}_L\right| \leq \bar{L}_L$, $\left|\bar{f}_M\right| \leq \bar{L}_{Mo}$, and $\left|\bar{f}_N\right| \leq \bar{L}_N$ in a reasonable flight envelope, the SMC/SMDO is designed in accordance with Eqs. (8.17)–(8.27) in the following steps:
Firstly, the components of the auxiliary vector-sliding variable $[s_L, s_M, s_N]^T$ are introduced

$$s_i = \sigma_i + z_i, \quad \dot{z}_i = \lambda_i - v_i, \quad i = L, M, N, \ \lambda_i = i \tag{8.60}$$

and the auxiliary vector-sliding variable dynamics are derived as

$$\dot{s}_i = \tilde{f}_i - v_i, \quad i = L, M, N \tag{8.61}$$

Secondly, the super-twisting injection terms are defined as in Eq. (8.54), and drive the auxiliary sliding variables s_i to zero in finite times, $i = L, M, N$. Therefore, the auxiliary injection terms v_L, v_M, and v_N exactly estimate the disturbances $\tilde{f}_L$, $\tilde{f}_M$, and $\tilde{f}_N$ in Eq. (8.61) in finite times, i.e.,

$$\tilde{f}_L = v_L, \ \tilde{f}_M = v_M, \ \tilde{f}_N = v_N \tag{8.62}$$

The disturbance estimates are fed into the virtual control laws in Eq. (8.49). Then, the obtained disturbance estimates in Eq. (8.62) are fed into the torque control laws in Eq. (8.59).

Control System Parameterization

The following choice of the controller (8.49), (8.51), (8.52), (8.53), (8.55), (8.59), (8.60), (8.61), and (8.62) parameters is recommended:

(a) $K_i > 0 \ \forall i = A_z, \phi, L, M, N$
(b) $K_i > K_j \ \forall i = L, M, N \ \forall j = A_z, \phi$
(c) $\frac{1}{\tau_i} > K_j \ \forall i = A_z, \phi, L, M, N \ \forall j = A_z, \phi$

Condition (a) is necessary for providing the asymptotic stability of sliding variable dynamics. Condition (b) enforces decoupling (time-scaling) between the inner-(σ_L, σ_M, σ_N) and the outer-loop (σ_{Az}, σ_ϕ) sliding variable dynamics given by Eqs. (8.33). Condition (c) provides for the transient times in the SMDO, which basically are controlled by the time constants of the filters in Eqs. (8.55) and (8.62). These transients are supposed to be faster than the transients in the control loops.

Meeting this condition helps to reduce the effect of the SMDO dynamics on the compensated dynamics of the tracking errors. All these conditions are not very restrictive and can be easily met in the RLV control system design.

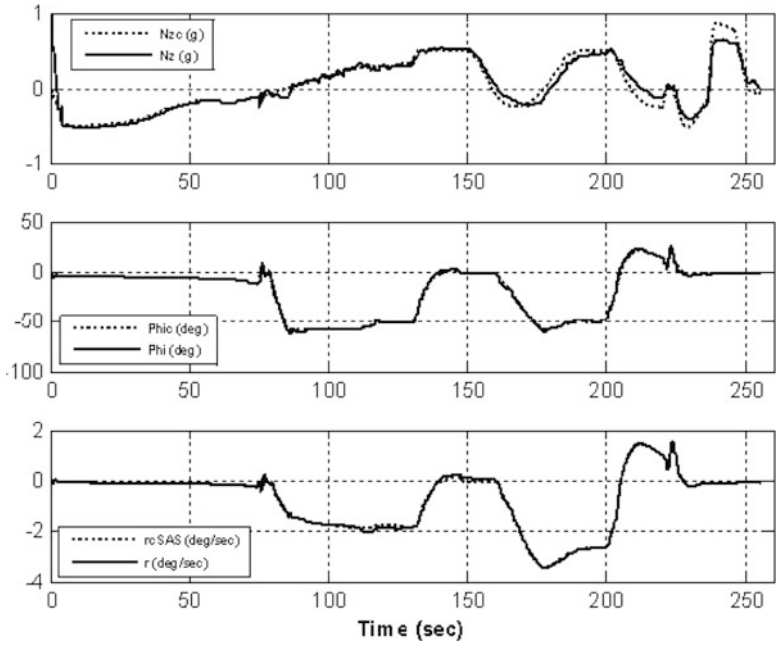

Fig. 8.2 Guidance command tracking: normal acceleration (*top*), roll angle (*center*), yaw rate (*bottom*), SMC/SMDO simulation, and nominal wind [104]

8.3.4 Flight Simulation Results and Analysis

The designed SMC/SMDO was coded and implemented in MATLAB/SIMULINK and the simulation results were compared with the baseline classical PID with gain-scheduling controller design. Only the autopilots were different between the two simulations; all other models remained unchanged, including a second-order actuator model with position and rate limiting and a wind model.

The simulations began at the TAEM interface and terminated at main gear touchdown on the runway. The control functions (8.59) in terms of roll, pitch, and yaw acceleration commands are transformed into virtual deflection commands by Eq. (8.47), allocated into actual actuator commands by means of the control allocator (8.48), and these are fed to the actuators (8.43) with deflection and rate limits being taken into account. The proposed continuous SMC/SMDO and the baseline controllers were compared in two simulation cases: one with a nominal wind and one with a severe headwind gust. Simulation results from the nominal wind case are shown in Fig. 8.2 through 8.5.

In comparing Figs. 8.2 (SMC/SMDO) and 8.3 (baseline), it can be seen that normal acceleration and roll angle tracking is far better with the SMC/SMDO (in particular, the roll angle command is followed almost perfectly). The yaw rate command is also followed very closely by the SMC/SMDO. The baseline controller

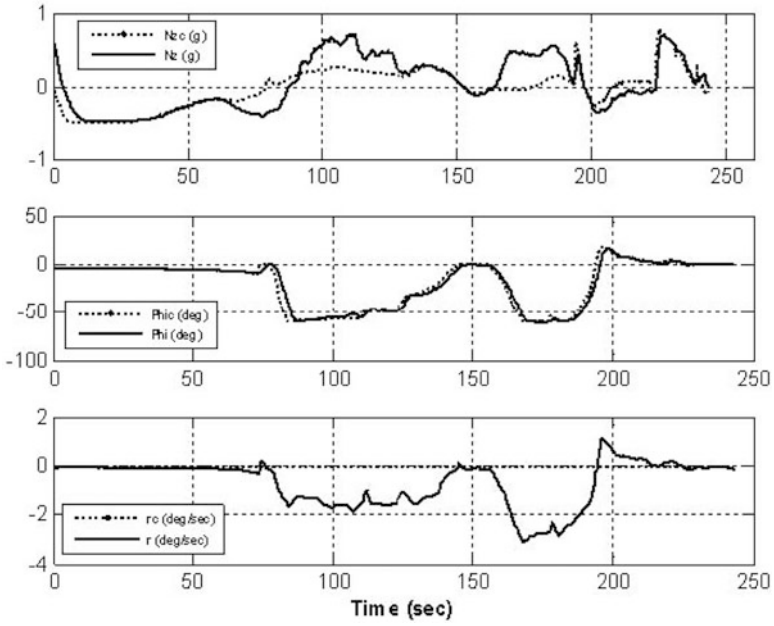

Fig. 8.3 Guidance command tracking: normal acceleration (*top*), roll angle (*center*), yaw rate (*bottom*), baseline simulation, and nominal wind [104]

does not follow the yaw rate command (which is always equal to zero, generated by the guidance loop) very well, due to the fact that it too uses turn coordination through interchannel cross-feeds. It is worth noting that the guidance command profiles are slightly different between the two simulations due to the fact that closed-loop guidance shapes its commands as a function of the flight condition and the distance from the landing site. The flight conditions differ because the two controllers produce different aero surface commands resulting in different aerodynamic accelerations on the vehicle. The aero surface deflections are shown in Figs. 8.4 and 8.5 for the SMC/SMDO and for the baseline controller respectively. The average deflections are similar in magnitude; however, in order to provide more accurate guidance command tracking, the SMC commands are more aggressive due to the use of the SMDO in response to maneuvers and other disturbances. This results in large transient deflections that quickly decrease once the tracking error is again close to zero.

To provide a more challenging case for the control system, a severe head-wind gust was simulated by artificially imposing a 25° angle of attack for a duration of 3 s, at 185 s flight time. The simulation results for this more stressing case are shown in Fig. 8.8 through 8.10. The gust appears as a step increase in angle of attack. Guidance command tracking is shown in Figs. 8.6 and 8.7 for the SMC/SMDO and baseline controller, respectively. At the time of the wind gust, the SMC/SMDO allows roughly 4g-error in normal acceleration, while roll and yaw errors are about

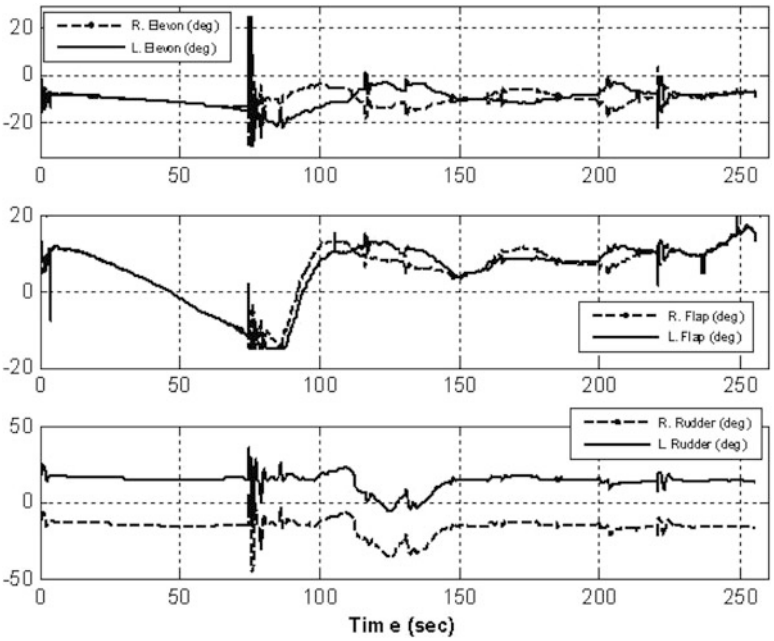

Fig. 8.4 Elevon (*top*), flap (*center*), and rudder (*bottom*) deflections, SMC/SMDO simulation, and nominal wind [104]

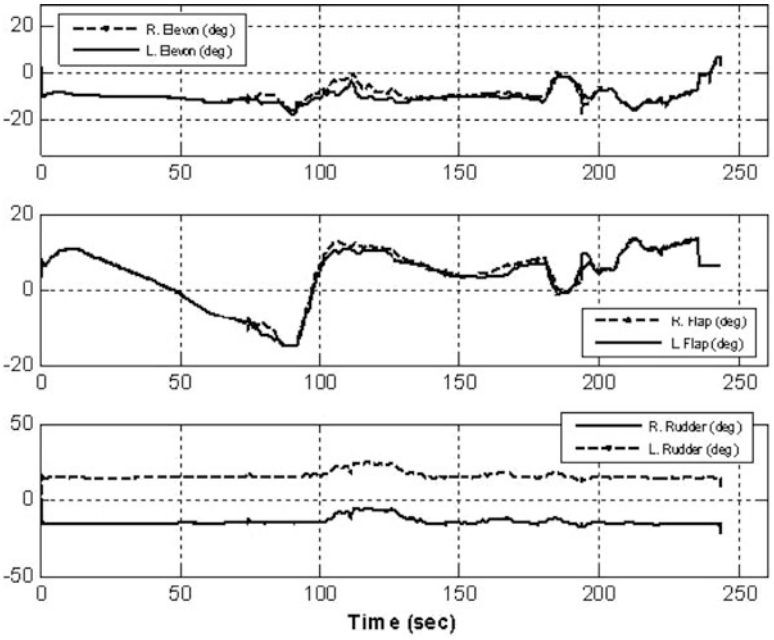

Fig. 8.5 Elevon (*top*), flap (*center*), and rudder (*bottom*) deflections, baseline simulation, and nominal wind [104]

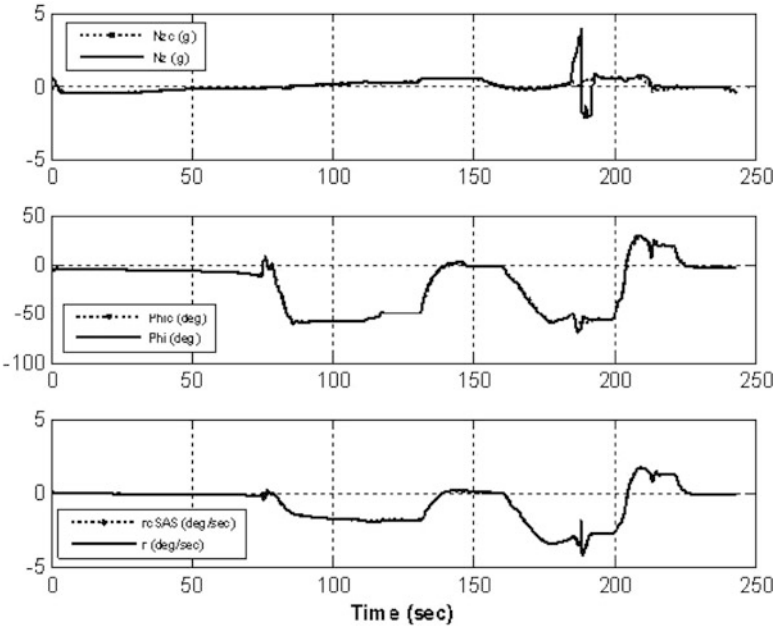

Fig. 8.6 Guidance command tracking: normal acceleration (*top*), roll angle (*center*), yaw rate (*bottom*), and SMC simulation with severe wind gust [104]

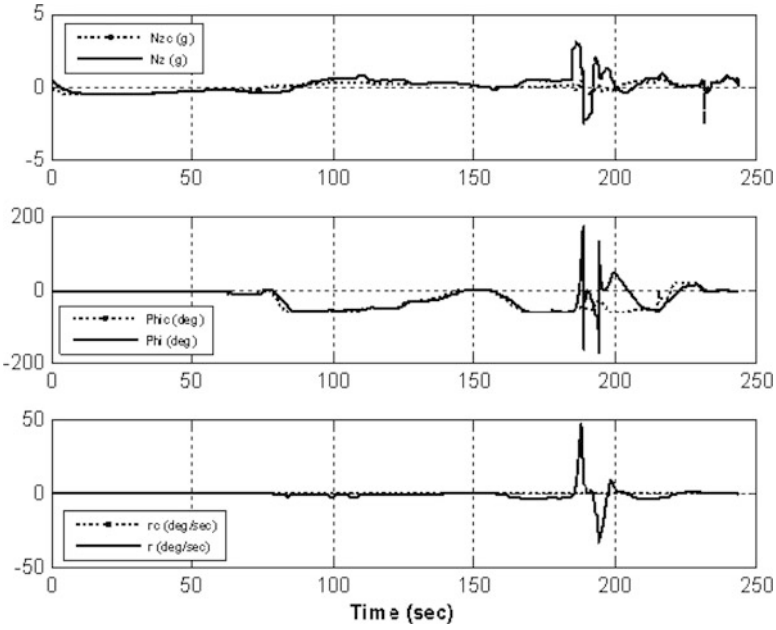

Fig. 8.7 Guidance command tracking: normal acceleration (*top*), roll angle (*center*), yaw rate (*bottom*), and baseline controller simulation with severe wind gust [104]

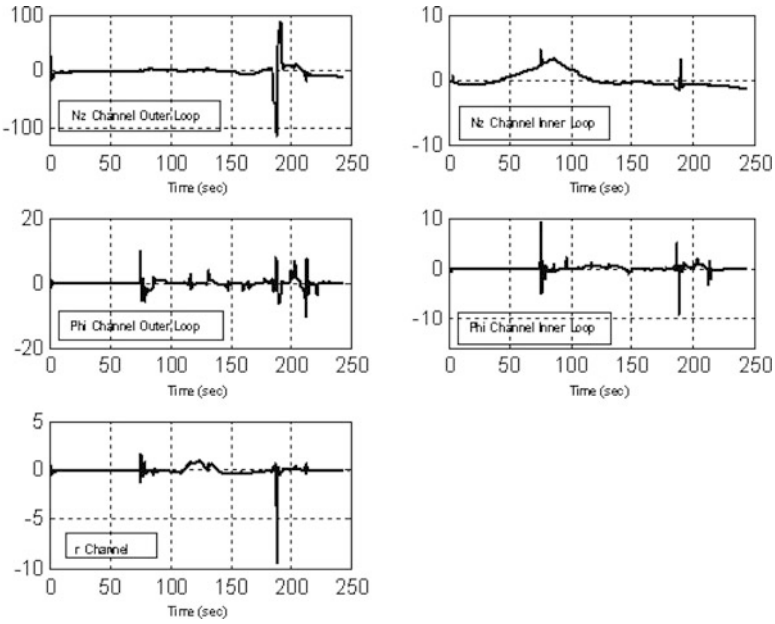

Fig. 8.8 Normal acceleration channel (Nz), roll channel (Phi), and yaw rate channel (r) SMC sliding variables and severe wind gust simulation [104]

the same as in the nominal simulation. In the baseline controller simulation, the vehicle rolls through 360° and the yaw rate climbs to a maximum of 50 degree per second. Figure 8.8 shows the sliding variables for the SMC/SMDO outer loop (8.50) and inner loop (8.56). Figure 8.9 shows the sliding variables for the SMDO outer loop (8.52) and SMDO inner loop (8.60). The sliding variables diverge occasionally due to the guidance maneuvers and the wind disturbance but then re-converge to a region around zero. The outer- and inner-loop SMDO disturbance estimates are shown in Fig. 8.10. The disturbance estimates are a function of maneuver rates, wind disturbances, and other unmodeled dynamics.

Remark 8.6. The proposed SMC/SMDO algorithm for the reusable launch vehicle flight control system was coded and implemented in the X-33 MAVERIC simulation. In its implementation, problems faced in real-world applications (like filtering and multi-rate subsystems) were successfully addressed.

8.4 Case Study: Satellite Formation Control

In this section we consider controlling the satellite formation, in particular, controlling the motion of one satellite as it follows a defined path around another satellite (that is orbiting the Earth). This tracking must be robust to model uncertainties

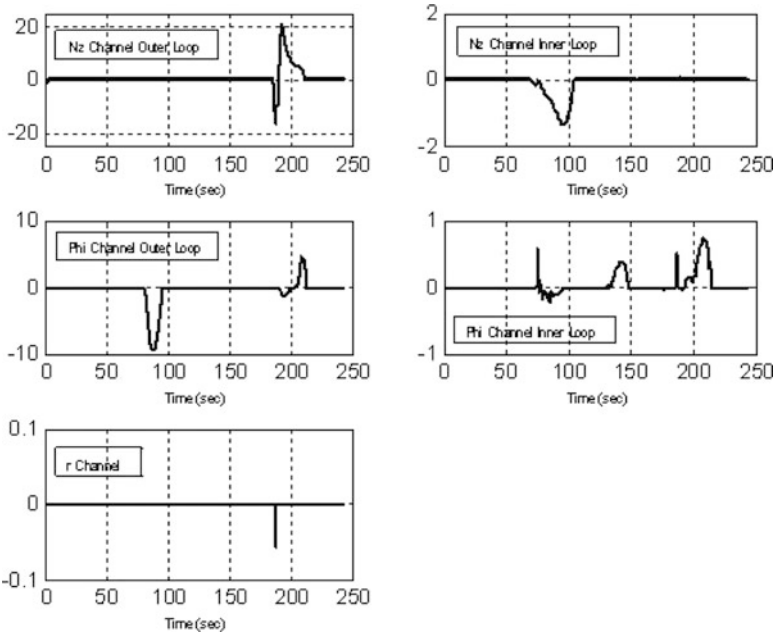

Fig. 8.9 Normal acceleration channel (Nz), roll channel (Phi), and yaw rate channel (r) SMDO sliding variables and severe wind gust simulation [104]

and external disturbances. The problem with any satellite formation control is that all orbiting bodies are subject to forces, which include gravitational perturbations, atmospheric drag, and solar radiation pressure, that tend to force the satellites out of their stable Keplerian orbits . Since the satellites are usually controlled by on–off thrusters, a conventional SMC with a dead-band is often used. The width of the dead-band usually is selected to minimize the fuel consumption. At the same time, simulations show that the jet-thruster duty cycle depends on a board computer step size. It means that using a dead-band controller does not permit controlling the frequency of switching. This could create a problem in using SMC in satellite formation control actuated by jet-thrusters that can be switched " on" and " off" only with a required duty cycle.

8.4.1 Satellite Formation Mathematical Model

The formation control problem studied in this section is a two-satellite formation. The coordinate system used is illustrated in Fig. 8.11.

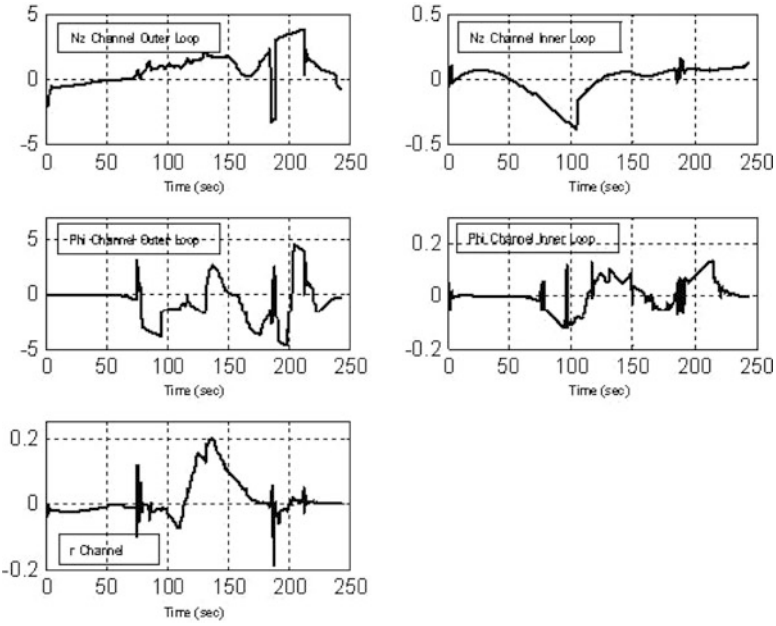

Fig. 8.10 Normal acceleration channel (Nz), roll channel (Phi), and yaw rate channel (r) SMDO disturbance estimates and severe wind gust simulation [104]

The first satellite, the leader, is in a circular orbit around a spherical Earth and for simplicity it is assumed to maintain that orbit in free flight. Assuming the second satellite is in a slightly elliptical orbit but remains close to the first when compared to the overall radii of their orbits around the Earth, we use the linearized Hill's equations to describe the relative motion between a leader and follower satellite. Since the available thrust levels are very low in many satellite applications, initial misalignments as well as transients resulting from disturbances may take many hours and even days to settle out. So, scaling the natural time t, a new time is defined such that $\tau = wt$, where w is the mean motion of the leader around the Earth (the value of the constant angular velocity that is required for a satellite to complete one revolution). The normalized Hill equations in the new time τ are

$$\begin{aligned} \ddot{x} - 2y - 3x &= u_x + d_x \\ \ddot{y} + 2\dot{x} &= u_y + d_y \\ \ddot{z} + \dot{z} &= u_z + d_z \end{aligned} \tag{8.63}$$

In Eq. (8.63) u_x, u_y, and u_z are the net (difference between leader and follower)-specific control forces acting on the follower satellite, and d_x, d_y, and d_z encompass the net-specific disturbances experienced by the two-satellite system, including linearization residuals. The specific control forces and disturbances are defined as

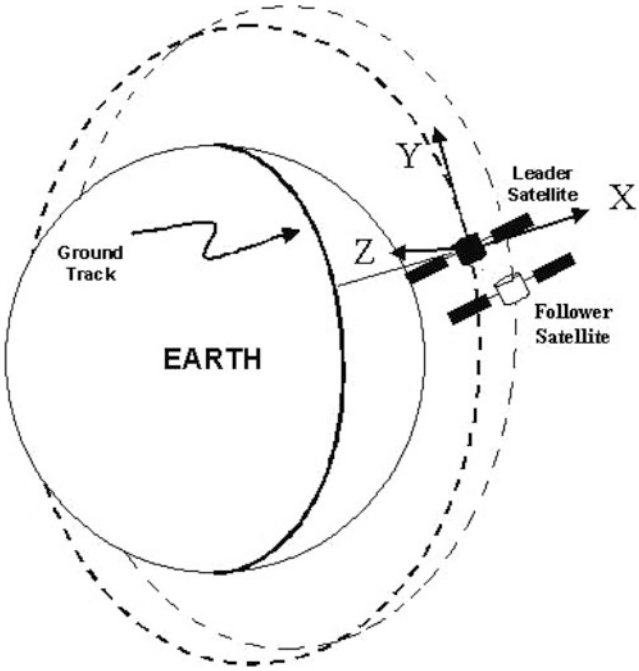

Fig. 8.11 Satellite formation coordinate system [139]

forces per unit mass per mean motion squared. All terms in Eq. (8.63) have a length dimension. The coordinates x, y, and z describe the position of the follower satellite relative to the leader satellite. Parameterizing Equation (8.63) as a function of τ with all external forces (control and disturbances) is equal to zero provides the reference trajectories for the simulation

$$x_c(\tau) = r\sin(\tau + \theta) \tag{8.64}$$

$$y_c(\tau) = 2r\cos(\tau + \theta) \tag{8.65}$$

$$z_c(\tau) = mr\sin(\tau + \theta) + 2nr\cos(\tau + \theta) \tag{8.66}$$

where r, m, n, and θ are arbitrary constants that define the elliptical desired path that the follower satellite maintains, relative to the leader in a force-free environment. In particular, r gives the size of the ellipse, θ is the initial angular position of the follower satellite on the path, and m and n are the slopes of the plane in which the path is located. For any given θ the follower satellite must enter the path (8.66) at initial conditions that are derived by setting $\tau = 0$ in Eq. (8.66), as well as in the derivative of Eq. (8.66), yielding

$$\begin{aligned} &x_c(0) = r\sin(\theta),\ y_c(0) = 2r\cos(\theta),\ z_c(0) = mr\sin(\theta) + 2nr\cos(\theta) \\ &\dot{x}_c(0) = r\cos(\theta),\ \dot{y}_c(0) = 2r\sin(\theta),\ \dot{z}_c(0) = mr\cos(\theta) - 2nr\sin(\theta) \end{aligned} \tag{8.67}$$

The value of θ defines the angle at which the follower satellite is making with a reference coordinate of the leader. Physically Equation (8.66) provides a circular or elliptical (depending on the choice of constants) reference trajectory around a leader satellite starting with the initial conditions defined in Eq. (8.67).

8.4.2 Satellite Formation Control in SMC/SMDO

If there is a mismatch between the follower satellite and the reference trajectory, then the starting point for the satellite will not be on one of the desired trajectories. Then a control system will be required to force the follower satellite back on track. The continuous SMC/SMDO controllers are supposed to achieve this goal while completely compensating for the bounded disturbances d_x, d_y, and d_z. Otherwise, the disturbances d_x, d_y, and d_z, which are due to the oblateness of the Earth, atmospheric drag, tesseral resonance, solar radiation pressure (so-called J_2 effects), and bulges of the Earth (so-called J_3 effects), will gradually disperse an uncontrolled formation. The J_2 effect is by far the dominant perturbation force compared to J_3. For this study, the representative d_x, d_y, and d_z disturbances are sine waves with a frequency of $0.6\,\mathrm{rad/s}(\tau)$ and are kept the same for all of the controllers studied. Also we assume that the leader satellite is maintained on the orbit by its own control.

Assuming the relative positions in Eq. (8.63) are measured, the vector-relative degree for this system is identified as $\bar{r} = [2, 2, 2]^T$ and the sliding variables (8.5) are formed as

$$\sigma = \left[\sigma_x, \sigma_y, \sigma_z\right]^T,\ \sigma_i = \dot{e}_i + c_{i,0}e_i + c_{i,-1}\int e_i d\tau\ \forall i = x, y, z \quad (8.68)$$
$$e_x = x_c - x,\ y_y = y_c - y,\ e_z - z_c - z$$

The integral terms in Eq. (8.68) are added in order to compensate for constant bias that could occur in the sliding modes at the implementation step. The following, optimized for fuel consumption, compensated dynamics of the output tracking errors in the sliding mode in a normalized time τ are

$$\sigma_i = \dot{e}_i + 1.8e_i + 1.0\int e_i \mathrm{d}\tau = 0 \rightarrow \ddot{e}_i + 1.8\dot{e}_i + e_i = 0\ \forall i = x, y, z \quad (8.69)$$

The SMC/SMDO of (8.17)–(8.25), (8.32), and (8.34) is designed ($u_i = v_i$ since $E(x,t) = I$ in Eq. (8.63)) for controlling the satellite formation model (8.63) and (8.66):

$$u_i = 10\sigma_i + \hat{v}_{ieq}\ \ \forall i = x, y, z \quad (8.70)$$
$$0.05\frac{\mathrm{d}\hat{v}_{ieq}}{\mathrm{d}\tau} = -\hat{v}_{ieq} + 2\mathrm{sign}(s_i)$$
$$s_i = \sigma_i + \int (u_i - 2\mathrm{sign}(s_i))\, d\tau$$

It is worth noting that the injection term v_i in the SMC/SMDO (8.70) can be also designed in a form of the super-twisting control as in Sect. 8.2.2.

8.5 Simulation Study

A Simulink model of the follower satellite motion around the leader was developed to test the effectiveness of the continuous SMC/SMDO algorithm in Eq. (8.70) against the set of disturbances. For this study, the representative disturbance is a sine wave with amplitude 0.5 km and a frequency of 0.6 rad/sec(τ).

The SMC/SMDO in Eq. (8.70) is compared with the conventional (discontinuous with dead-band) SMC. The same orbital period is used, i.e., 100.7 m. Recall that τ is defined as the product of the mean motion and time. Therefore, for a 100.7 m orbit, the actual time required to reach $\tau = 1$ is 961.6 s. For the simulations an Euler first-order integration algorithm is used, and the time step is fixed at 0.01 ms.

In Eq. (8.66) the values of the parameters are taken as $r = 0.5$ km for the reference trajectory, whereas $r = 0.6$ km for the follower satellite in order to create the initial condition offset. Also $n = 0$ and $m = \sqrt{3}$ are defined to set the follower satellite in a circular orbit around the leader at $\pm\frac{2\pi}{3} rad$ inclination with the x-axis. The angular position $\theta = \frac{\pi}{2}$ is the same for both the reference trajectory and the simulated satellite's trajectory. A pulse-width-modulation (PWM) technique is used to turn the continuous SMC/SMDO signals into a pulse train that could be realizable by a satellite on–off jet-thruster. It is assumed that the thruster can cycle at a frequency of 10 Hz. Due to the 961.6 s(τ) conversion factor, 10 Hz signal in the t time domain would need to be approximately a $10000\, cycles/\tau$ signal in the τ domain. Therefore, a dither signal, a sine wave of 10000 cycles/τ with amplitude of $0.25 \cdot 10^{-5}$ km/s^2, is combined with the control signal to model the required duty cycle of the thrusters. In order to further optimize weekly fuel consumption, the dead-zone is used in the relay elements of PWM. The recommended dead-band optimal value is taken as $\delta_i = 0.5 \cdot 10^{-5}$km/s^2 and the corresponding PWM with a dead-band is shown in Fig. 8.12.

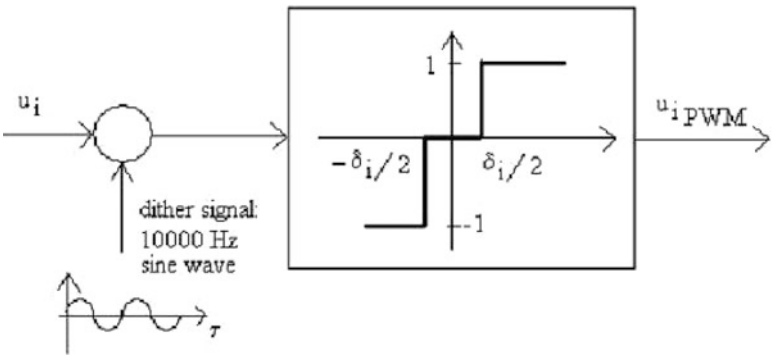

Fig. 8.12 PWM with dead band [139]

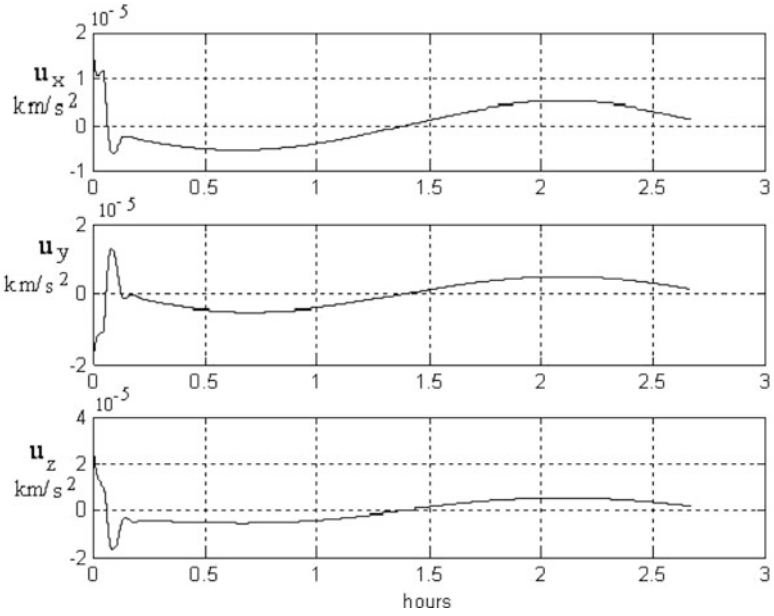

Fig. 8.13 Continuous SMC/SMDO (km/s^2) [139]

Figure 8.13 shows the control inputs to the follower satellite while using the continuous SMC driven by the SMDO. After a few hours, this control drives the sliding variables and the errors to near zero. However, since this algorithm is supposed to be controlling a satellite thruster that fires pulses of thrust of constant magnitude, the continuous control input shown in Fig. 8.13 versus the original time is not very useful.

Figure 8.14 shows the control inputs with the PWM technique implemented in the original time t.

Here, the 10 Hz duty cycle is clearly illustrated. With the PWM technique, all continuous SMC reduce the errors between reference trajectory and the follower satellite's trajectory to near zero. The upper boundaries of steady-state errors are compared in Table 8.1.

It can be seen that the SMC/SMDO provides more accurate stabilization compared to conventional SMC. Figure 8.15 shows a 3-dimensional view of the relative motion between the leader and follower satellite using the continuous SMC/SMDO with the PWM technique incorporated.

The corresponding weekly fuel consumptions in terms of ΔV, which are low for both methods, are shown in Table 8.2

Remark 8.7. The studied SMC/SMDO easily drives the control on–off thrusters with given duty cycle using the PWM technique, which is an improvement over a conventional (discontinuous with dead-band) SMC. The simulation analysis shows

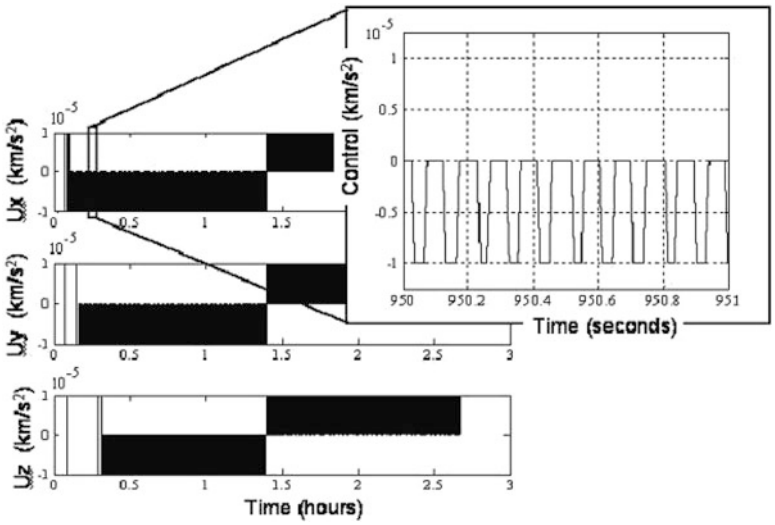

Fig. 8.14 Continuous SMC/SMDO modulated by PWM [139]

Table 8.1 Steady-state stabilization errors

Method	Conventional SMC	SMC/SMDO
$\|e_x\|\ (km)$	3.610^{-4}	1.510^{-5}
$\|e_y\|\ (km)$	3.410^{-4}	0.410^{-5}
$\|e_z\|\ (km)$	3.710^{-4}	2.810^{-5}

that the continuous SMC/HOSM algorithm is effective in reducing the tracking errors of the follower satellite in the presence of a bounded disturbance function while keeping fuel consumption at a low level. It also appears that the PWM technique introduced does not degrade the tracking performance to any significant degree retaining fixed duty cycle.

8.6 Notes and References

For details about vector and total relative degree, see, for example, [112]. It is worth noting that the problem formulated in Sect. 8.1 can be also addressed for systems with stable zero dynamics [112].

The equation for finite-time-convergent compensated dynamics given in Sect. 8.1.2 is taken form [23].

The model of the RLV is from [106] and [190]. The multiple-loop asymptotic SMC design algorithm used for the RLV is from [104]. The overall stability analysis of the double-loop SMC/SMDO is also from [104].

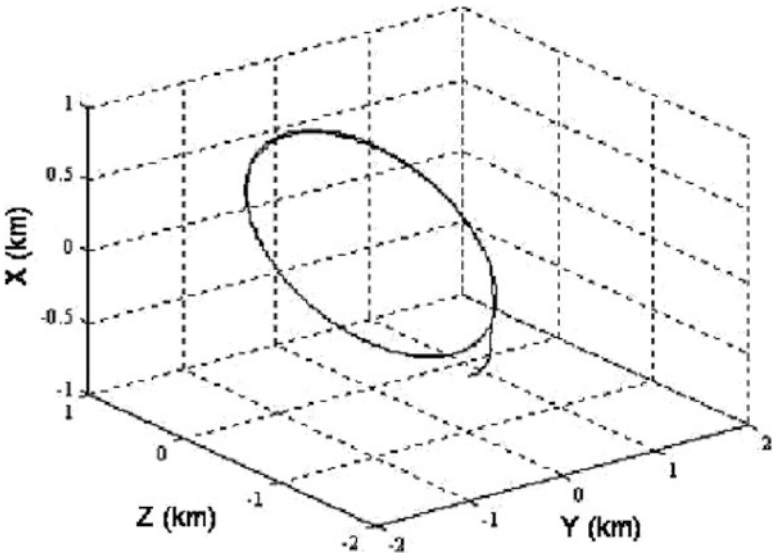

Fig. 8.15 Three-dimensional trajectory: continuous SMC/SMDO modulated by PWM (km) [139]

Table 8.2 The weekly fuel consumption

Method	Conventional SMC	SMC/SMDO
$\Delta V_x\ (m/s)$	0.212	0.210
$\Delta V_y\ (m/s)$	0.203	0.202
$\Delta V_z\ (m/s)$	0.203	0.202

The description of the Keplerian orbits and the satellite fuel consumption problems are from [194]. The continuous SMC/SMDO robust controller, realized by PWM to provide a required duty cycle in the control command to the jet-thrusters and used to robustly control the satellite formation while providing low weekly fuel consumption, is reported in [139]. An analysis of the application of a broader variety of SMC/SMDO techniques to the satellite formation control problem, including a super-twisting disturbance observer and a continuous robust SMC based on integral sliding surface design, can be found in [139].

The challenging task of output tracking in systems with transmission zeros located in the right-hand side of the complex plane or, generally speaking, in systems with unstable zero dynamics, is called a nonminimum phase output tracking problem [112]. A solution to the nonminimum phase output tracking problem using sliding modes, for an aerospace example, can be found in [160]. Output tracking in nonminimum phase systems with arbitrary relative degree, using higher-order sliding mode control, is studied in [102, 164, 167].

The 2-SM controllers that are applied to the launch vehicle and missile system are discussed in [163, 165, 176]. Other aerospace applications of SMC/HOSM control and disturbance observation techniques appear in a special issue of the Journal of Franklin Institute [169].

8.7 Exercises

Exercise 8.1. Consider the following linear system subject to external disturbances:

$$\dot{x} = Ax + B(u + \varphi)$$
$$y = Cx$$

where $u \in^2$ is the control input and φ is an external disturbance

$$A = \begin{bmatrix} 1 & -1 & 0 \\ 0 & -3 & 1 \\ -1 & 0 & -2 \end{bmatrix},\ B = \begin{bmatrix} 0\,0 \\ 1\,0 \\ 0\,1 \end{bmatrix},\ \varphi = \begin{bmatrix} 3 + 4\sin(t) + \cos(4t) \\ x_1 + 4\cos(t) + \sin(3t) \end{bmatrix},$$
$$C = \begin{bmatrix} 0\,1\,0 \\ 0\,0\,1 \end{bmatrix}$$

The vector-function φ is assumed to be unknown and is used for computer simulation only. Design a continuous decoupled SMC/SMDO that achieves asymptotic tracking $y \to y_c$ with a given settling time $t_s = 0.5\,\text{s}$, when $y_c = \left[\cos(t), \sin^2(t)\right]^T$, and $x(0) = [1, -2, 3]^T$. Support the simulation results by plotting the corresponding variables.

Exercise 8.2. Repeat Exercise **8.1** and design a finite-time SMC/SMDO that achieves tracking $y \to y_c$ with an overall given convergence time $t_r = 0.5\,\text{s}$.

Exercise 8.3. Consider Chua's circuit (Example 2.7) with an output $y = x_1$. The unknown function $f(x_1) = -x_1(1 - x_1^2)$ is used for simulation purposes only. Design a continuous SMC/SMDO that achieves asymptotic tracking $y \to y_c$ with a given settling time of $t_s = 1.5\,\text{s}$. Simulate the control system with

$$y_c(t) = 10 + \sin^2 t\ (V),\ x(0) = [0.5, 0.4, 0.2]^T$$

Support the simulation results by plotting the corresponding variables.

Exercise 8.4. Repeat Exercise **8.3** and design a finite-time SMC/SMDO that achieves tracking $y \to y_c$ with a given convergence time of $t_r = 1.5\,\text{s}$.

Exercise 8.5. The dynamics of an armature-controlled DC motor are given by

$$\begin{cases} J\frac{d\omega}{dt} = k_m i - T_L \\ L\frac{di}{dt} = -iR - k_b\omega + u \\ y = \omega \end{cases}$$

where J is the moment of inertia, i is armature current, L and R are armature inductance and resistance, respectively, ω is the motor angular speed, k_b is a constant relating to back electromotive force, k_m is a motor torque constant, T_L

is load torque, and u is a control function in terms of the armature voltage. Design a sliding mode control u that drives $y = \omega \to y_c$ as time increases, assuming that $y = \omega$ is measurable. Assume all the parameters are known except for the load torque T_L that is assumed to be bounded together with its derivative: $|T_L| \leq L_m$, $\left|\dot{T}_L\right| \leq \bar{L}_m$ Design a continuous SMC/SMDO that achieves asymptotic tracking $y \to y_c$ with a given settling time t_s. Simulate the control system with $R = 1\,\text{Ohm}$, $L = 0.5\,\text{H}$, $k_m = 5{\cdot}10^{-2}\,\text{N}\cdot\text{m/A}$, $k_b = k_m$, $J = 10^{-3}\,\text{N}\cdot\text{m}\cdot\text{s}^2/\text{rad}$, $T_L = 10\cos(3t)\,\text{N}\cdot\text{m}$, $y_c(t) = 60 + 50\sin(2t)$, $t_s = 1.2\,\text{s}$, $\omega(0) = 10\,\text{rad/s}$, and $i(0) = 0$. Support the simulation results by plotting the corresponding variables.

Exercise 8.6. Repeat Exercise **8.5** and design a finite-convergent-time SMC/SMDO that achieves tracking $y \to y_c$ with an overall given convergence time $t_r = 1.2\,\text{s}$.

Exercise 8.7. A simplified model of the dynamics of the longitudinal motion of an underwater vehicle is given by

$$m\ddot{x} + k\dot{x}\,|\dot{x}| = u + T_d$$
$$y = x$$

where x is the position of the vehicle, u is the control function (a force that is provided by a propeller), m is the mass of the vehicle, $k > 0$ is the drag coefficient, and T_d is an unknown smooth disturbance bounded together with its derivative. Assuming the value of m is known exactly, the drag coefficient is bounded $k_1 \leq k \leq k_2$ and the position and its derivative (velocity) x, $\dot{x}$ are measured, design a continuous SMC/SMDO that drives $y \to y_c$ as time increases, with given settling time t_s. Simulate the control system for $x_1(0) = 2\,\text{m}$, $x_2(0) = 0.5\,\text{m/s}$, $m = 4\,\text{kg}$, $t_s = 5\,\text{s}$, $k = 1.5 + 0.4\sin(2t)\left[\frac{kg}{m{\cdot}s}\right]$, $T_d = 10^4 + 10^3\sin(t)$, and

$$y_c(t) = \begin{cases} 0.1t^2, if\ 0 \leq t \leq 10\,\text{s} \\ 10 + 2\,(t - 10)\,, if\ t > 10\,\text{s} \end{cases}$$

Support the simulation results by plotting the corresponding variables.

Exercise 8.8. Repeat Exercise **8.7** and a finite-convergent-time SMC/SMDO that achieves tracking $y \to y_c$ with an overall given convergence time $t_c = 3s$.

Exercise 8.9. The evolution of the angle of attack of a missile controlled by fin deflection can be described by a simplified system of differential equations

$$\begin{cases} \dot{\alpha} = q - 2.7\alpha + d(t) \\ \dot{q} = -5.5\alpha - 0.4q - 19\delta \\ \dot{\delta} = -20\delta + 20u + 20h(t) \\ y = \alpha \end{cases}$$

where α, δ are angle of attack and fin deflection in rad, respectively; q is pitch rate in rad/s, u is the control function in rad, and $\mathrm{d}(t)$ and $h(t)$ are smooth bounded disturbances in rad/s. The angle of attack and pitch rate are measured. Design a continuous double-loop SMC/SMDO that drives $y \to y_c$ as time increases with given settling time t_s. Take pitch rate q as a "virtual" outer-loop control and u as the inner-loop control. Simulate the control system for $\alpha(0) = 0$, $q(0) = 0$, $\delta(0) = 0$, $h(t) = 0.1\sin(t)$ rad/s, $h(t) = 0.05\cos(2t)$ rad/s, $t_s = 0.3$ s, and

$$\alpha_c(t) = \begin{cases} 0.5\sin(0.5t), & if \ \ 0 \le t \le \pi \\ 0.5, & if \ t > \pi \end{cases}$$

Support the simulation results by plotting the corresponding variables.

Exercise 8.10. Repeat Exercise **8.9** and design a single-loop finite-convergent-time SMC/SMDO that achieves tracking $y \to y_c$ with an overall given convergence time $t_c = 0.25s$.